JOURNAL OF MATERIALS SCIENCE **39** (2004) 4185–4192

Nano-scratch study of pulsed laser-deposited hydroxyapatite thin films implanted at high energy with N^+ and AR^+ ions

H. PELLETIER*, V. NELEA, P. MILLE
Laboratoire d'Ingénierie des Surfaces, Institut National des Sciences Appliquées, 24, Bld. de la Victoire, F-67084 Strasbourg, France
E-mail: pelletier@mail.insa-strasbourg.fr

D. MULLER
Laboratoire PHASE, CNRS, UPR 292, 23 rue de Loess, BP 20CR, F-67037 Strasbourg, France

In this study we report a method to improve the adherence of hydroxyapatite (HA) thin films, using an ion beam implantation treatment. Crystalline HA films were grown by a pulsed laser deposition technique (PLD), using an excimer KrF* laser. The films were deposited at room temperature in vacuum on Ti-5Al-2.5Fe alloy substrates previously coated with a ceramic TiN buffer layer and then annealed in ambient air at (500–600)°C. After deposition the films were implanted with N^+ and Ar^+ ions accelerated at high energy (1–1.5 MeV range) at a fixed dose of 10^{16} cm^{-2}. The intrinsic mechanical resistance and adherence to the TiN buffer layer of the implanted HA films have been evaluated by nano-scratch tests. We used for measurements a spherical indenter with a tip radius of 5 μm. Different scratch tests have been performed on implanted and unimplanted areas of films to demonstrate the effects of N^+ and Ar^+ ion implantation process on the films properties. Results show an enhancement of the dynamic mechanical properties in the implanted zones and influence of the nature of the implanted species. The best results are obtained for films implanted with nitrogen. The modes of failure of the films under loading are described.

1. Introduction

Hydroxyapatite (HA) ceramics are continuously studied in order to develop new bioactive and osteoconductive bone prostheses [1]. HA coatings are currently produced in the form of thin films on titanium alloys prostheses. In spite of excellent biocompatibility, HA films suffer from poor mechanical properties (hardness, elastic modulus and adherence).

In a previous work [2], we have studied the mechanical response of pulsed laser deposition HA films grown on Ti alloy substrate with or without a buffer layer. We have experimentally proved that the samples with a buffer interlayer (TiN, ZrO_2 or Al_2O_3) are completely crystalline and present better mechanical characteristics. However, the intrinsic mechanical properties of HA films (hardness and elastic modulus) are not yet satisfactory. During indentation steps on the load-displacement curves correlated with the lack in density concentration of pores through the HA film thickness were observed [3]. Thus, we have decided to treat pulsed laser deposited HA films grown on titanium alloy with a TiN interlayer by implantation with Ar^+ ions at high energy (about 1.5 MeV) [4]. We provide evidence of an enhancement of the mechanical characteristics due to the effects of ion bombardment resulting in pores elimination and recrystallization.

The aim of the present work is to investigate the influence of implanted species on HA film densification. The HA/TiN/Ti-alloy multi-layer system was modified after deposition by nitrogen implantation with a high energy of 1 MeV at low dose (about 10^{16} cm^{-2}).

Compared to the previous study [4], the mechanical properties have been estimated using a nanoindentation apparatus in scratch test mode equipped with a spherical tipped indenter having a 5 μm tip radius. The scratch tests have been performed in different conditions of applied load to cover a wide range of dynamic solicitations.

2. Experimental procedure

We used for deposition a typical PLD installation consisting of a KrF* ($\lambda = 248$ nm, $\tau_{FWHM} \geq 20$ ns) excimer laser source and a stainless steel vacuum chamber evacuated down to 10^{-4} Pa residual pressure. The laser beam was focused at 45° on a hot pressed pellet

*Author to whom all correspondence should be addressed.

obtained from high purity polycrystalline HA powder (for more details, see the Ref. [5]). Polished disks cut from Ti-5Al-2.5Fe (TiAlFe) alloy bars were used as substrates. Prior to deposition the titanium alloy substrates were coated with a ceramic TiN buffer layer. This layer was grown also by PLD starting from a stoichiometric TiN target in a low pressure atmosphere (10^{-1} Pa) on substrates heated at 650°C temperature. During HA deposition, the TiN–Ti alloy bilayer system was kept at room temperature. The films were subsequently annealed in air at 550°C for 1 hour with both a heating and cooling rate of 2°C/min. The HA films had a thickness of ∼1 μm, while the thickness of the TiN buffer layer varied between 200–500 nm.

The samples were implanted with N^+ (sample 1) and Ar^+ (sample 2) ions using a Van de Graaff-type implanter [6]. The implantation was carried out at a constant dose of 10^{16} cm^{-2} with energies of 1.5 and 1 MeV for argon and nitrogen atoms, respectively. The current density was kept constant at 1 μAcm^{-2}. In order to choose the proper energy for the HA/TiN/TiAlFe composite, we performed ion distribution simulations using the TRIM® numeric code [7]. According to the LSS model [8], the theoretical projection can be described by the estimated range (R_P) and its standard deviation (ΔR_P) of the implanted atoms. The calculated values of R_P and ΔR_P for the used implantation parameters depending of the estimated density of the HA coatings (varying from 1.5 to 3.15 g cm^{-3}) are given in Table I.

Scratch tests were performed with a spherical diamond indenter having a 5 μm radius. The instrument used was a Nano Indenter® XP (MTS, Nano Innovation Center, Oak Ridge, TN) which has an available load range of 20 μN–500 mN. The resolution and other measurement parameters of this apparatus can be found in Ref. [9]. The diamond tip was drawn across the film surface at a constant scratching velocity (V) of 10 μms^{-1} under progressively loads increasing from 1 to 10 mN (scratch #1) and from 5 to 25 mN (scratch #2), respectively. The scratch length (L) was maintained constant at 500 μm and the loading rate ($\dot{P}$) during the scratch test can be defined as following:

$$\dot{P} = \frac{V}{L} \times (P_2 - P_1) \tag{1}$$

Moreover, around the interface between the unimplanted and implanted zones, the diamond tip was drawn across the sample region under constant loads 5 ± 0.5 mN (scratch #3) and 25 mN (scratch #4), with a scratch length of about 1000 μm.

Scratch testing is one of the more frequently used experimental methods for determining the mechanical resistance of coatings. It is a relatively quick and efficient way for acquiring information on the dominant damage mechanisms of a coating.

During scratching a normal (P) load was applied and generated tangential forces (F_T) are measured (Fig. 1a). The apparent coefficient of friction can be estimated:

$$\mu_0 = \frac{F_T}{P} \tag{2}$$

The indentation depth (h) can be calculated from the curve of the initial scratch recorded at very low load (about 30 μN), representing the sample roughness (noted 1 in Fig. 1b) and the curve of the scratch test performed at a desired conditions (noted 2 in Fig. 1b):

$$h = |h_T - h_i| \tag{3}$$

The scratch (dynamic) hardness (H_d) which is a mean of the contact pressure between the indenter and the material can be estimated from the curves shown in Fig. 1b. For such multi-layer systems, the dynamic hardness is computed in first approximation with the following formula:

$$H_d = \frac{2P}{\pi a^2} \tag{4}$$

with the contact radius $a = \sqrt{2Rh - h^2}$.

We have chosen a spherical indenter to determine mechanical properties of implanted PLD HA films, although this kind of tip geometry is not well adapted to characterize surface of materials with a gradient of mechanical properties, such as bilayer systems (film on substrate) or multilayer systems (implanted surface, whose mechanical properties are directly related to the concentration distribution of implanted atoms [10]). The average values of strain (ε) and of the strain rate ($\dot{\varepsilon}$) beneath the indenter spherical are expressed as [11, 12].

$$\varepsilon = 0.2\frac{a}{R} \tag{5}$$

$$\dot{\varepsilon} = \frac{V}{b} \tag{6}$$

Thus, during the scratch test with increasing applied load, the strain and strain rate vary with indentation depth, as well as the mechanical properties of the analyzed material.

We can encounter some difficulty extracting the intrinsic properties of films or treated surfaces using a spherical tip. In this study, we are interested in qualitative values to compare the mechanical values of the unimplanted and implanted zones for the same sample. We use here macroscopic parameters to evaluate the benefit of implantation on the properties of PLD HA films, such as the resistance to penetration curve, indentation depth (h, nm) versus the indenter tip displacement (d, μm). With the nanoindentation apparatus

TABLE I Evolution of the theoretical projection as a function of implantation parameters

	Ar^+ implantation at 1.5 MeV		N^+ implantation at 1 MeV	
HA film density (g/cm^{-3})	Projected ion range R_p (μm)	Standard deviation ΔR_p (μm)	Projected ion range R_p (μm)	Standard deviation (μm) ΔR_p
1.5	1.34	0.16	1.77	0.15
2.5	1.08	0.15	1.53	0.13
3.15	0.81	0.14	1.15	0.21

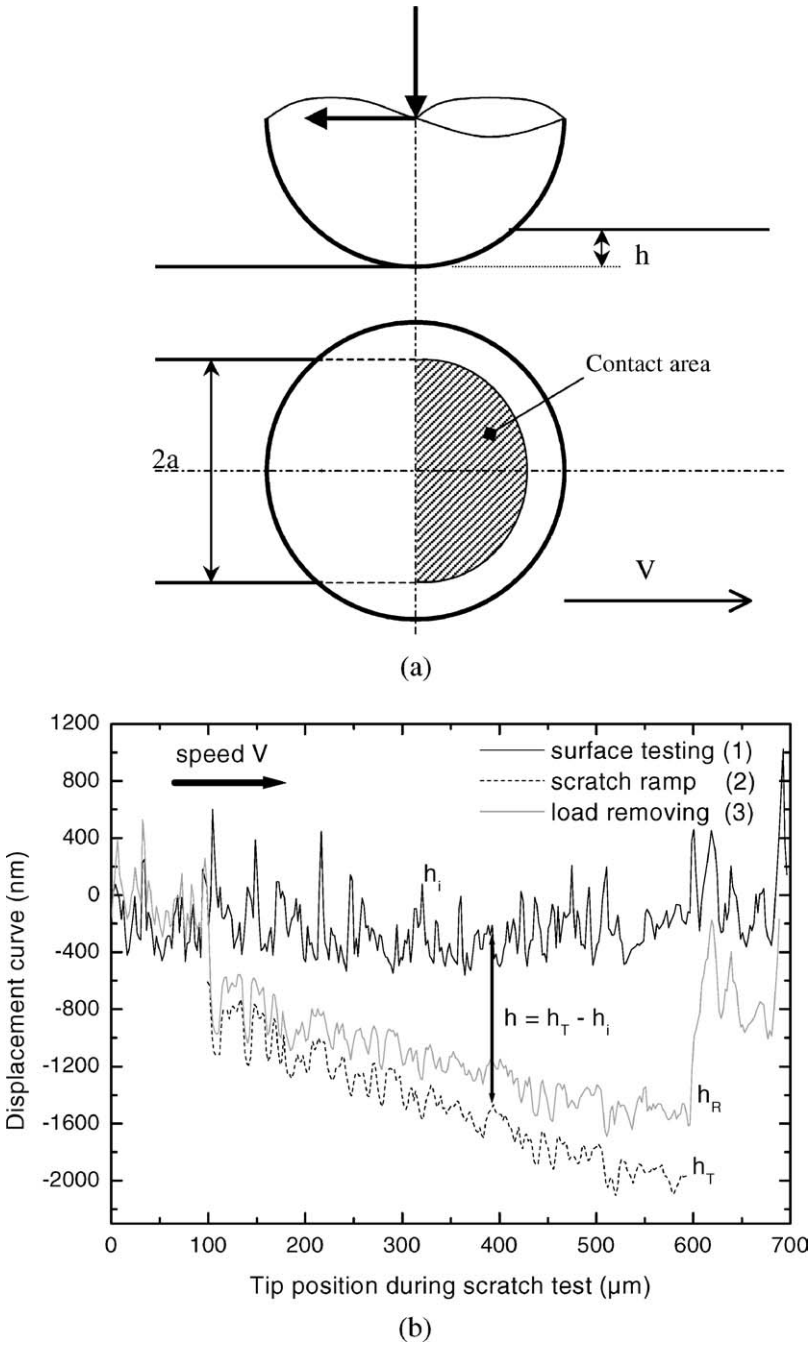

Figure 1 Description of the contact between the spherical indenter and the surface of a material during a scratch test (a) and example of recorded data obtained after an experimental scratch test at increasing load on the unimplanted region (b).

in the scratch mode, we try to reproduce the mechanical degradation generated by an abrasive particle. Thus, the curves (h) vs. (d) can be related in first approximation to the abrasive wear resistance of PLD films. Moreover, compared to Berkovich tip geometry [4], we think the spherical tipped indenter to be more sensitive in the same load range. The three Berkovich edges create rapid plastic deformation, even at low loads. The direct consequence is that the Berkovich tip cut rapidly through the HA film and reached the first interface between the PLD HA film and the TiN underlying layer.

3. Results and discussion

The nanoindentation tests in normal static mode [13] show that the mechanical properties of the PLD HA films implanted with nitrogen seem to be homogeneous through the implanted zone. We have then performed scratch tests in the center of the implanted region of sample 1 with increasing load (scratch #1 and #2). The curves, h vs. d, plotted in Fig. 2 correspond to the resistance to penetration, respectively, for unimplanted and implanted zones. The solid line curves represent the experimental data recorded by the nanoindentation apparatus, whereas the dot line curves are only tendencies to show clearly the difference between the two zones. First, we can note that the oscillations as a function of the penetration depth are higher in the unimplanted zone. The frequency and almost the scattering are directly related with the initial roughness. In the unimplanted zone, the oscillations of penetration depth are very important even at low applied load ($P \leq 10$ mN),

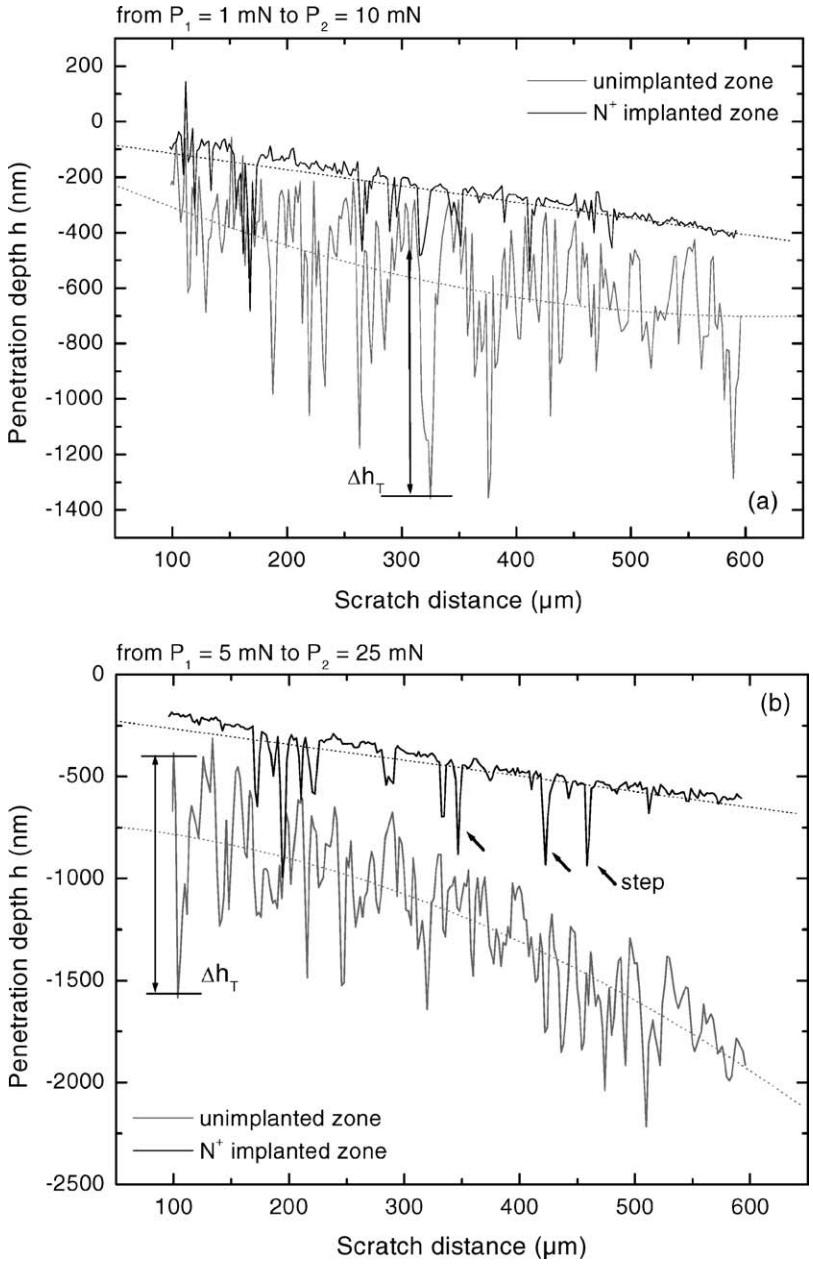

Figure 2 Resistance to penetration after N^+ implantation for scratch tests #1 (a) and #2 (b).

with variations Δh_T of about 1000 nm, corresponding to the average thickness of the HA layer (see Fig. 2b).

In Fig. 4, we have represented the initial topography measured by the first scratch for test #3 and #4 performed at constant load around the interface. We can note that the surface topography is quite different between the two zones and the roughness parameters may be smaller in the implanted region. The tendency curves (linear and polynomial fits for the implanted and unimplanted zones, respectively) show clearly the benefit produced by ion beam treatment after deposition. The difference in mechanical behavior is much more important at high load (Fig. 2b). In the unimplanted zone, the spherical indenter goes rapidly through the HA layer to reach the TiN layer. However, in the implanted zone, the HA layer seems to mechanically withstand tip displacement and the deformation mechanism occurs only in the implanted HA layer.

To illustrate the beneficial effect of nitrogen implantation, we utilized scratch tests at constant applied load (scratch #3 and #4 in Table II) in the near interfacial region between the unimplanted and implanted zones. The scratch tests start in the unimplanted area and the spherical tip is then moving progressively at constant speed in the direction of the implanted region. The spherical tip goes across three zones with distinct

TABLE II Experimental parameters used for scratch tests

No. scratch	Scratch length L (μm)	Velocity V ($\mu m \cdot s^{-1}$)	Starting scratch load P_1 (mN)	Maximum scratch load P_2 (mN)	Loading rate ($mN \cdot s^{-1}$)
#1	500	10	1	10	0.18
#2	500	10	5	25	0.40
#3	1000	10	4.5	5.5	0.01
#4	1000	10	24.5	25.5	0.01

TABLE III Mechanical properties of unimplanted and implanted areas determined by scratch test

Sample	Area	P (mN)	h_{AV} (nm)	a (nm)	Strain (%)	Strain rate (s^{-1})	H_d (GPa)	μ_0 ($a.u.$)
1	unimp.	5	682	2521	10	1.98	0.50	0.25
1	N^+ imp.	5	333	1794	7	2.79	0.99	0.28
2	unimp.	5	688	2531	10	1.97	0.49	0.24
2	Ar^+ imp.	5	301	1708	6.8	2.92	1.09	0.26
1	unimp.	25	1263	3322	13	1.50	1.44	0.26
1	N^+ imp.	25	830	2759	11	1.81	2.09	0.32
2	unimp.	25	790	2697	11	1.85	2.18	0.28
2	Ar^+ imp	25	409	1980	8	2.52	4.05	0.31

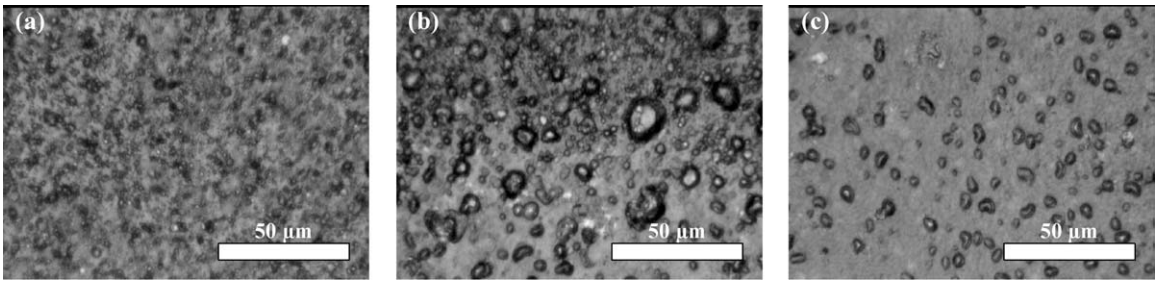

Figure 3 Optical micrograph of (a) unimplanted zone A, (b) interface between the two zones B and (c) N^+ implanted zone C.

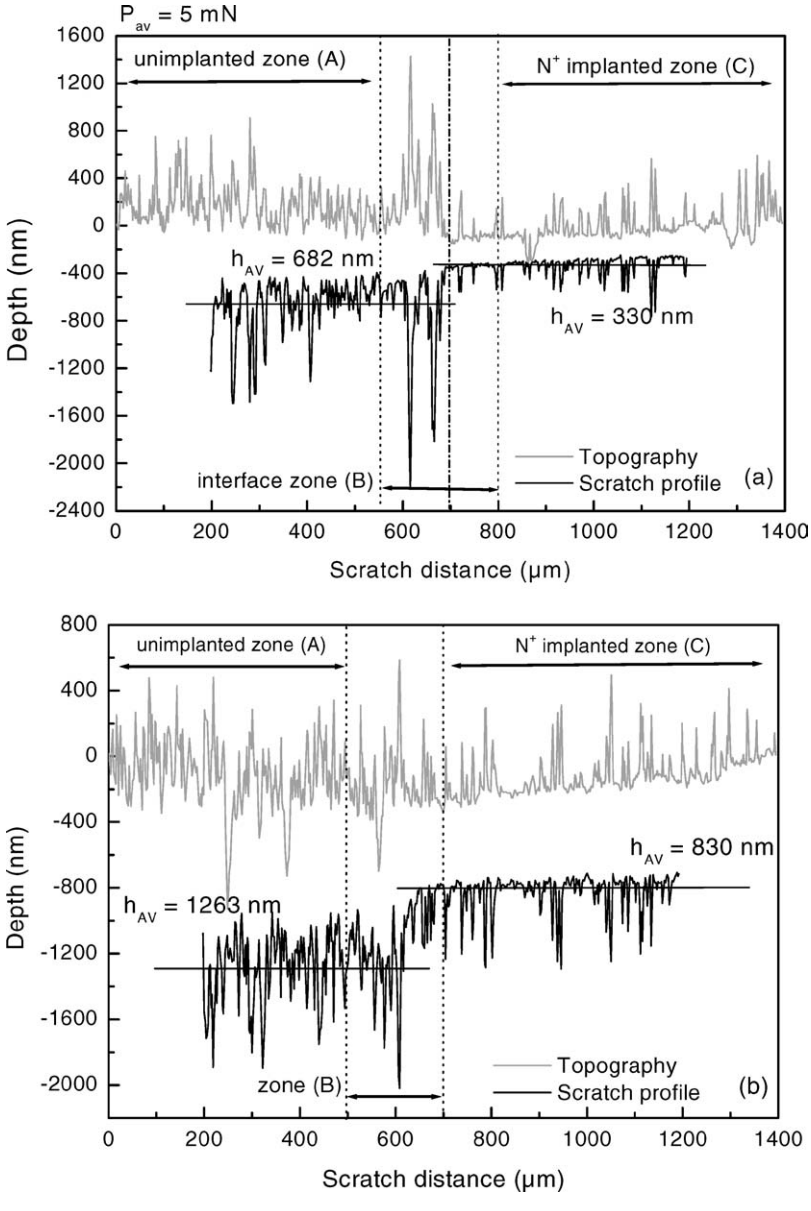

Figure 4 Resistance to penetration after N^+ implantation for scratch tests #3 (a) and #4 (b).

morphology, as we can see with optical microscopy in Fig. 3. The different zones are respectively marked by zone A (Fig. 3a), zone B (Fig. 3b) and zone C (Fig. 3c). The difference in morphology can also be distinguished in Fig. 4 on the initial scratch performed to estimate the topography of the indented surface. The interface zone B is located between 550 and 800 μm in Fig. 4a. We can observe a quick variation of the initial roughness, which is in good correlation with the optical micrograph (see Fig. 3b).

In Fig. 4a and b, the penetration curves (black solid line) show a step when the spherical tip crosses the interface between the unimplanted and implanted zones. For the scratch test performed at 5 mN, the penetration depth is at least divided by a factor 2. Moreover, in the implanted zone, the oscillations of penetration depth are reduced, proving an increase of HA layer density, and then of mechanical properties, as we can see in Table III.

The dynamic hardness (H_d) has been calculated with Equation 6, with average values of penetration depth h_{AV} (i.e., contact radius a) estimated with the recorded experimental data in Fig. 4, for each zone. We have given the average values of strain and strain rate to be able to compare the hardness values. For the unimplanted zone, we can note that the hardness value is constant for a given load. The nitrogen implantation treatment at a low applied load increases the hardness by a factor of 2.

In the case of argon implantation treatment of PLD films, the same phenomena are observed. However, as demonstrated in a normal static indentation test [13], the HA layer implanted with argon is not homogeneous and isotropic, exhibiting important variations of the mechanical behavior as a function of the indented zone. We have performed scratch tests in two different zones on the Ar^+ implanted part. In Fig. 5 we notice that the mechanical response of the HA layer after im-

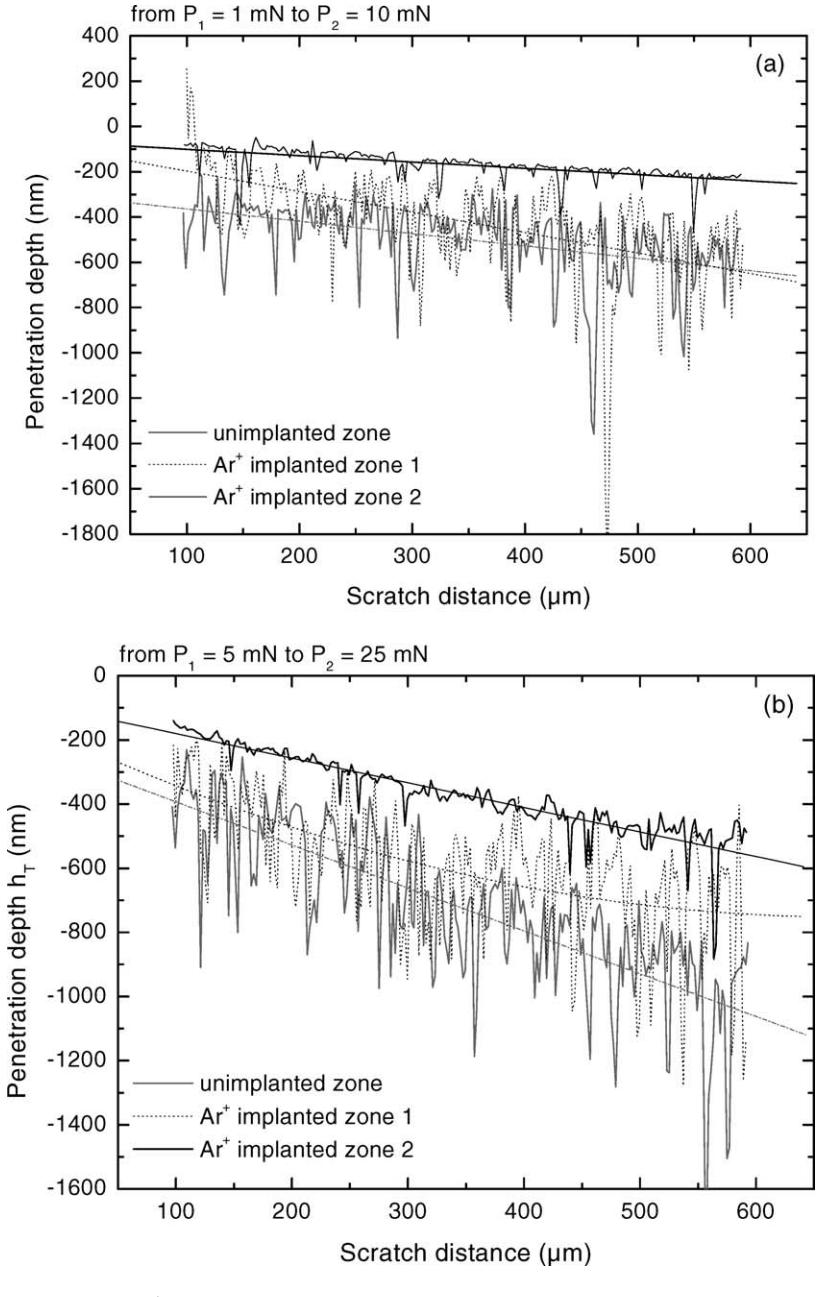

Figure 5 Resistance to penetration after Ar^+ implantation for scratch tests #1 (a) and #2 (b).

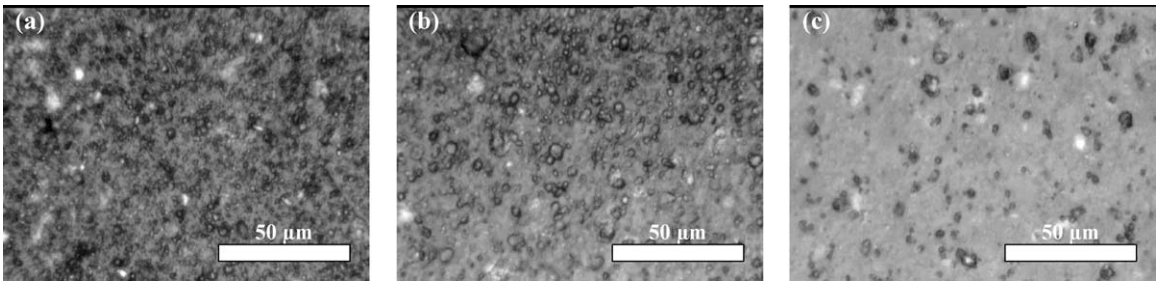

Figure 6 Optical micrograph of (a) unimplanted zone A, (b) interface between the two zones B and (c) Ar^+ implanted zone C.

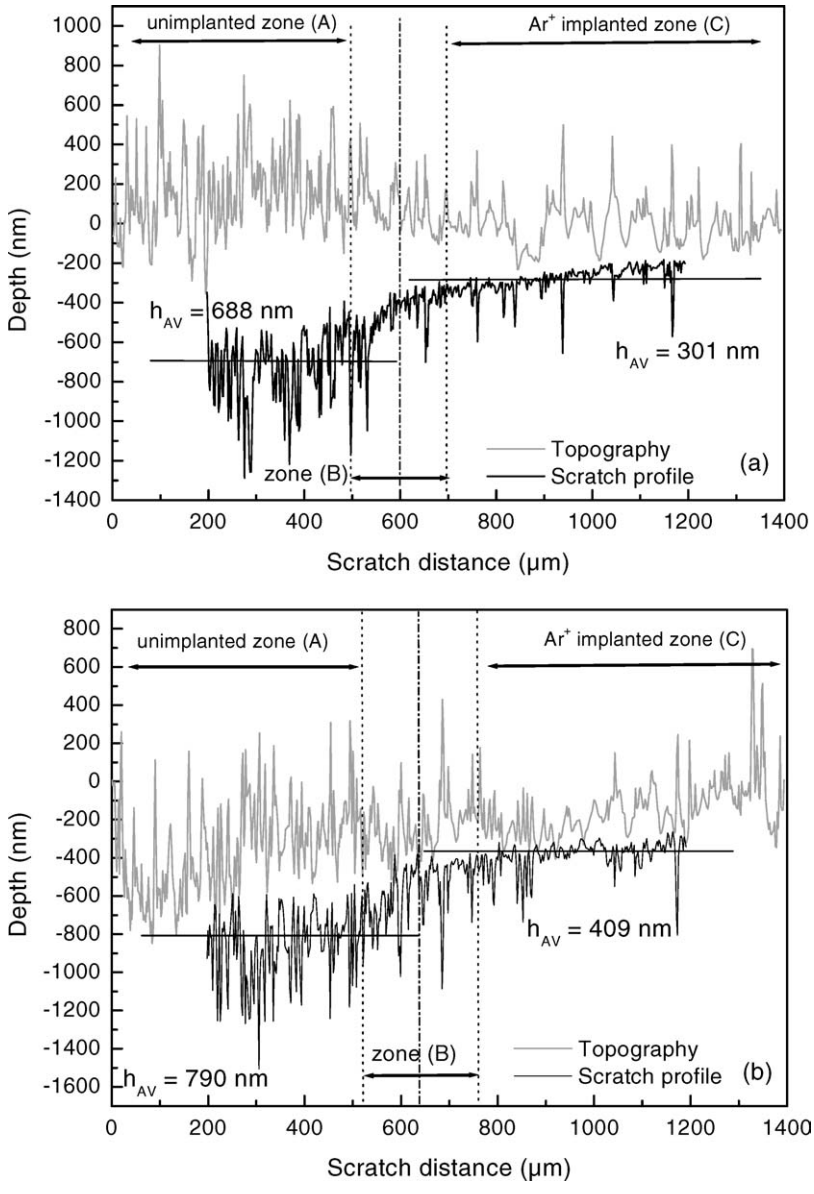

Figure 7 Resistance to penetration after Ar^+ implantation for scratch tests #3 (a) and #4 (b).

plantation depends on the location of the scratch. The resistance to penetration curve of the implanted zone noted 1 in Fig. 5 (black dot line) is similar to the one of the unimplanted zone (gray solid line). A small difference is observed for high load ($P \geq 15$ mN), when the spherical tip approaches the interface between the HA layer and the TiN buffer layer. We think that this difference can be correlated with the presence of Ar in the HA layer. Indeed, according to TRIM simulation (see Table I) as a function of the layer density and for penetration depth greater than 700 nm, the tip is penetrating into the argon concentration distribution. For the implanted zone noted 2 in Fig. 5, the increase of the resistance to penetration can be compared to the one observed after nitrogen implantation (see Fig. 3). In this Ar^+ implanted zone, the obtained curve h vs. d is smooth, with some steps, corresponding to the initial roughness.

Like sample 1 implanted with nitrogen, we have performed scratch tests at constant load around the

interface between the unimplanted and implanted zones. By optical microscopy we can define three distinct zones with different morphologies (Fig. 6). Compared to nitrogen implantation (Fig. 4), the variation of measured penetration depth is more progressive during the scratch test. We do not observe a distinct step on the penetration curve (Fig. 7), as noted for nitrogen implantation. However, according to Table III, the variation of dynamic hardness H_d, as calculated with average values of indentation depth, is similar to the one determined after nitrogen implantation, with an increase of a factor of 2.

In Table III we have reported the average values of apparent friction coefficient measured with nanoindentation during scratch test. The apparent friction coefficient is defined by the ratio between the tangential force and the normal load (Equation 3), but, in fact, this parameter is not the same as the local Coulomb's friction coefficient [14]. The apparent coefficient can be divided into two components, a ploughing part and an adhesive part. This parameter is thus very sensitive to the initial roughness of the surface. Moreover, in order to extract the Coulomb's friction coefficient, the two parts may be computed using analytical expressions (not done here). In the unimplanted zones, we observe strong oscillations of the apparent friction coefficient (μ_0) as a function of the indenter tip displacement, directly related to the topography. For each analyzed sample, we note an increase of μ_0 with increasing applied load. This evolution can be explained by the fact that the apparent friction coefficient depends on the strain and the strain rate, by contrast with the Coulomb's coefficient friction, assumed to be constant. For scratch tests performed with normal loads of less than 10 mN, Table III shows that there is no difference between the unimplanted and the implanted zones for each ion species, with a μ_0 value in the range of 0.24 to 0.28. For higher loads the apparent coefficient friction appears to be greater in the Ar^+ and N^+ implanted zones, with average values greater than 0.3. We suppose that the observed evolution with the normal applied load (i.e., with indentation depth) is directly related to the improvement of the density and the toughness of the HA layer after nitrogen and argon implantation, yielding to an increase of the tangential force applied by the layer on the indenter tip during scratch test. According to the definition of the apparent friction coefficient, we can conclude that the implantation treatment improves the ploughing resistance of the HA layer. This feature can be very interesting for tribological applications, such as biomedical applications, especially for orthopedic prosthesis.

Other experimental studies (RBS, TEM, GIXRD) are in progress in order to understand the hardening mechanism, which is mainly, according to us, related to the ion beam mixing around the interface, generated by the collisions between the incident particles (N^+ and Ar^+) and the target atoms (Ca, P, O, Ti), and the increase of dislocations density.

4. Conclusion

This experimental study has shown that implantation treatment may be a good process to improve the mechanical properties of thin films, like PLD HA coatings largely used in biomedical applications. The improvement observed using scratch tests performed with a spherical indenter in different conditions can be correlated to the Ar^+ and N^+ implantation treatment. Indeed, for all calculated parameters (resistance to penetration, dynamic hardness and apparent friction coefficient), the difference between the unimplanted and implanted zones are more important for large applied loads, when the indentation depth is near the implanted region, around the interface between the HA layer and the buffer TiN layer. These results prove that implantation improves the abrasive wear resistance of the HA layer, leading to an important increase of the lifetime of the biomedical prosthesis.

References

1. H. ZENG, W. R. LACEFIELD, and S. MIROV, *J. Biomed. Mater. Res.* **50** (2000) 248.
2. V. NELEA, C. RISTOSCU, C. CHIRITESCU, C. GHICA, I. N. MIHAILESCU, H. PELLETIER, P. MILLE and A. CORNET, *Appl. Surf. Sci.* **168** (2000) 127.
3. V. NELEA, H. PELLETIER, I. ILIESCU, J. WERCKMANN, V. CRACIUN, I. N. MIHAILESCU, C. RISTOSCU and C. GHICA, *J. Mater Sci. Mater in Med.* **13** (2002) 1167.
4. V. NELEA, H. PELLETIER, D. MULLER, N. BROLL, P. MILLE, C. RISTOSCU and I. N. MIHAILESCU, *Appl. Surf. Sci.* **186** (2002) 483.
5. V. NELEA, PhD thesis, University of Strasbourg (ULP) France, 2002.
6. J. P. STOQUERT, J. J. GROB and D. MULLER, *Nucl. Instr. Meth.* B **79** (1993) 664.
7. U. LITTMARK and J. F. ZIEGLER, *Phys. Rev.* **23A** (1981) 64.
8. J. LINDHARD, N. SCHARFF and H. E. SCHIOTT, *Mater. Fys. Medd. Dam. Vid. Selsk.* **14** (1963) 33.
9. W. C. OLIVER and G. M. PHARR, *J. Mater. Res.* **7**(6) (1992) 1564.
10. H. PELLETIER, P. MILLE, A. CORNET, J. J. GROB, J. P. STOQUERT and D. MULLER, *Nucl. Instr. Meth.* B **178** (2001) 319.
11. J. S. FIELD and M. V. SWAIN, *J. Mater. Res.* **8**(2) (1993) 297.
12. J. BUCAILLE, E. FELDER and G. HOCHSTETTER, Wear **249** (2001) 422.
13. H. PELLETIER, V. NELEA, P. MILLE and D. MULLER, Mechanical Properties of Pulsed Laser-Deposited Hydroxyapatite Thin Film Implanted at High Energy with N^+ and Ar^+ Ions. Part I Nanoindentation with Spherical Tipped Indenter, in submision.
14. J. L. BUCAILLE, E. FELDER and G. HOCHSTETTER, *J. Mater. Sci.* **37** (2002) 3999.

Received 29 July 2003
and accepted 18 March 2004